Measurement induced entanglement phase transition

Zhaoyou Wang
Department of Applied Physics, Stanford University, Stanford, CA 94305
(Dated: June 24, 2020)

Submitted as coursework for PH470, Stanford University, Spring 2020

Unitary dynamics typically drives a closed many-body system towards larger entanglement, eventually saturating at a volume-law scaling for the entanglement entropies of subsystems. On the other hand, local measurements could disentangle local degrees of freedom from the rest of the system and therefore reduce the amount of entanglement. Recently it has been demonstrated that an entanglement phase transition exists at some critical measurement rate. Below that rate, the system exhibits volume-law entanglement and above that rate the system becomes area-law entanglement. In this work, we reproduce the measurement induced entanglement phase transition with an 1D hybrid random Clifford circuit model. We also extend the model to 2D as well as all-to-all coupling to explore how the critical measurement rate changes with the dimension of the system. At higher dimensions, the random unitaries are better at generating entanglement due to the increased connectivity and therefore intuitively the critical measurement rate should be higher than 1D. Indeed our results suggest a higher critical measurement rate at 2D as well as the absence of entanglement phase transition with all-to-all coupling.

I. INTRODUCTION

Quantum entanglement has been the essential concept behind many modern understanding of condensed matter physics[1], especially for characterizing many-body ground states[2–5]. Time evolution of entanglement entropy also reveals universal behavior and provides new insights into many-body dynamics out of equilibrium[6–11]. For thermalizing phases the entanglement entropy grows linearly in time and saturates with a volume law[8], while for many-body localized systems it shows a slow logarithmic growth[6,7]. Practically, entanglement growth typically determines the complexity of simulating many-body quantum dynamics classically[12], while the ability to generate and manipulate entanglement is also crucial for quantum computation.

Even though unitary dynamics tends to evolve towards higher entanglement, local degrees of freedom under projective measurements will disentangle from the rest of the system and therefore reduce the amount of entanglement. Remarkably, the competition between unitary dynamics and local measurements could lead to an entanglement phase transition, where below a critical measurement rate the system exhibits volume-law entanglement and above that rate the system becomes area-law entangled[13–15]. From a quantum computing perspective, such a competition widely exists in the near-term noisy quantum devices where the depth of quantum circuits are limited by the amount of noise in the system[16]. Studying such measurement induced entanglement phase transition may also shed light on new schemes of quantum error correction as well as future supremacy experiments[17].

In this work, we numerically demonstrate the entanglement phase transition for 1D random unitary circuits with measurements. We also explore how the phase transition behaves at higher dimensions by investigating 2D models as well as all-to-all coupling models.

II. MODEL DESCRIPTION

Consider a hybrid random unitary circuit with both local unitaries and measurements for L qubits arranged on an one-dimensional chain (Fig. 1). The unitary evolution is decomposed into multiple layers with each layer formed by a sequence of non-overlapping two-qubit gates acting on either all odd bonds or all even bonds. Every two adjacent layers are defined as one discrete time step. More specifically, layer t implement the unitary (ignore measurements here)

$$U^{(t)} = U^{(t)}_{\text{even}} U^{(t)}_{\text{odd}} = \left(\prod_{x \text{ even}} U^{(t)}_{x,x+1} \right) \left(\prod_{x \text{ odd}} U^{(t)}_{x,x+1} \right). \tag{1}$$

Therefore after time t the state will evolve under $|\psi(t)\rangle = U^{(t)} |\psi(t-1)\rangle$. The total time steps T will be large enough so that steady state could be reached.

The measurements happen between unitary layers and each qubit is measured independently with probability p. Notice here measurements could be performed between $U^{(t)}_{\text{even}}$ and $U^{(t)}_{\text{odd}}$ within the same time step t. Since all two-qubit gates are random, the measurements are assumed to be performed along Z axis without loss of generality. In other words, with probability $1-p$ nothing happens

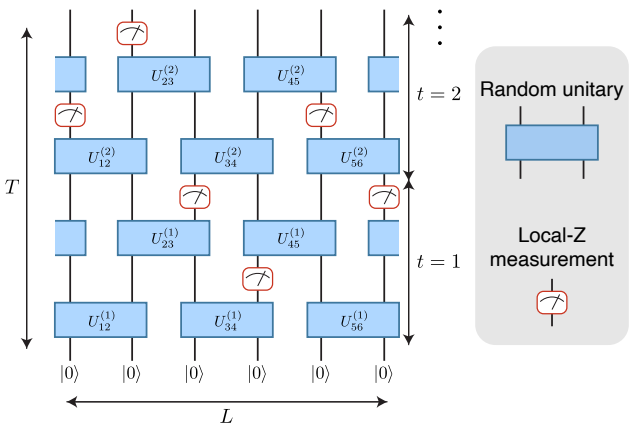

FIG. 1: Random unitary circuit with measurements. The initial state is assumed to be a product state and the unitary layers act on all the odd and even bonds in an interleaving fashion. The total time steps T is chosen to be large enough so that steady state is reached and random local projective measurements in the Z basis could independently happen at any site in space and time with probability p.

and with probability p a single qubit will be projected to $|0\rangle$ or $|1\rangle$ and gets disentangled from the rest of the system.

We should mention that the model here works in the framework of quantum trajectory, which unravels the mixed state time evolution. Basically after each measurement the state is randomly projected to another pure state instead of tracking all possible outcomes with a density matrix. Therefore all results are averaged over the three sources of randomness in this model: random unitaries, random measurement positions and random outcomes of the projective measurements.

A. Clifford circuit

In order to simulate larger system sizes, all unitaries are sampled independently from the uniform distribution over the two-qubit Clifford group, instead of from the Haar measure on $U(4)$. By definition, Clifford unitaries do not generate any entanglement in the operator space: they simply map products of Pauli operators to another products of Pauli operators. Therefore by tracking the operators' time evolution instead of the wavefunction, Clifford circuits could be simulated efficiently on a classical computer as proved by Gottesman–Knill theorem[18]. Furthermore, random Clifford circuits approximate well the random Haar circuits and both could generate volume law entanglement entropy[9,19].

1. *Entanglement entropy*

To quantify the amount of quantum entanglement in the steady state, we calculate the set of Rényi entropies,

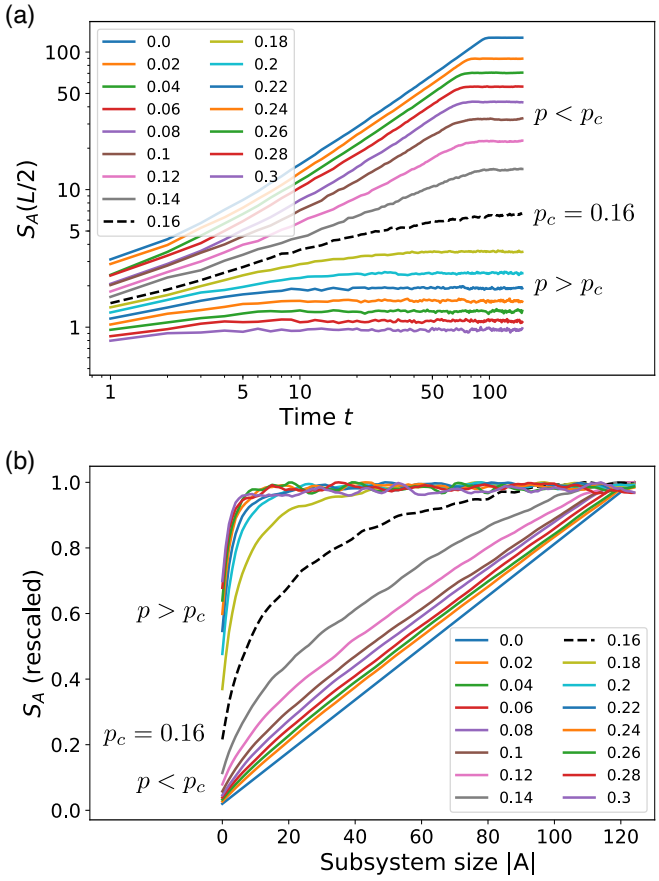

FIG. 2: (a) Time evolution of the entanglement entropy S_A in the middle of the system, with subsystem A consisting of sites $1 \sim L/2$. (b) Rescaled steady state entanglement entropy S_A as a function of the subsystem size $|A|$ for different measurement rates p. For better visualization, each curve is rescaled linearly by the maximum entropy at that measurement rate, so that after rescaling the maximum entropy for different p will always be 1. In both plots, the legend gives the measurement rate p for each line and the black dashed line represent the critical rate $p_c \approx 0.16$. The simulations are done with $L = 256$ qubits and total time steps $T = 150$ for reaching steady state.

defined as

$$S_n(A) = \frac{1}{1-n} \log \mathrm{Tr}[\rho_A^n], \quad n \geq 0 \tag{2}$$

where the L qubits are bipartitioned into subsystems A and B and ρ_A is the reduced density matrix $\rho_A = \mathrm{Tr}_B |\psi\rangle \langle\psi|$. In the limit of $n \to 1$, Rényi entropy becomes the von Neumann entropy.

For any state generated by the random Clifford circuit considered here, ρ_A will always have a flat entanglement spectrum, meaning that all its non-zero eigenvalues are equal to each other. In this case, all Rényi entropy are also equal to each other and we will drop the Rényi index n from now on.

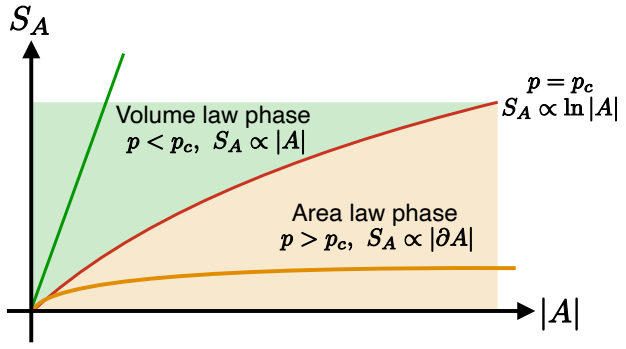

FIG. 3: Phase diagram and the leading order scaling of steady state entanglement as a function of the measurement rate p. Figure adapted from "Measurement-driven entanglement transition in hybrid quantum circuits", by Yaodong Li, Xiao Chen, and Matthew PA Fisher, *Physical Review B*, 98(20):205136, 2018[14].

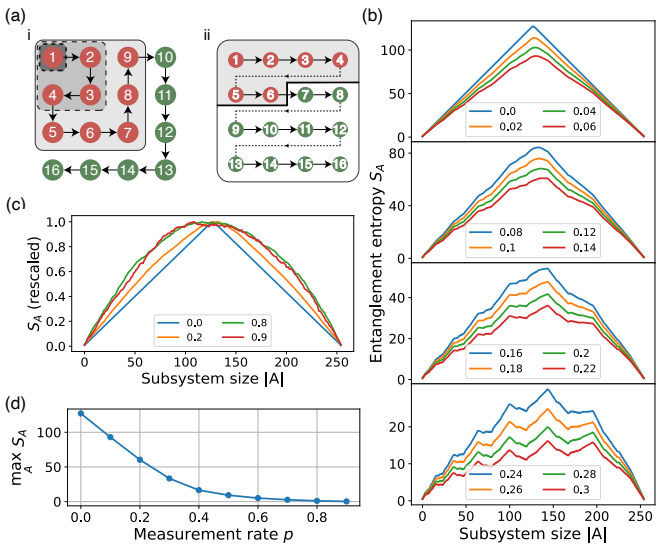

FIG. 4: (a) i) Spiral mapping and ii) raster scan mapping of a 2D lattice into 1D string for evaluation of entanglement entropy. (b) Steady state entanglement entropy S_A as a function of $|A|$ along the 1D string mapped with spiral ordering in (a) i). At low measurement rates, the symmetric feature around $L = 128$ comes from a volume law entanglement while at high measurement rates the zigzag pattern represents a 2D area law with the spiral ordering. (c) Rescaled S_A versus $|A|$ for a system with all-to-all random unitary coupling at different measurements p. Same as Fig. 2 (b), each curve is rescaled linearly by the maximum entropy at that measurement rate, so that after rescaling the maximum entropy for different p will always be 1. (d) Maximal S_A for the all-to-all coupling model as a function of the measurement rate p. In other words, this is the linear rescaling factor used in (c).

2. *Simulation algorithm*

The simulation algorithm is based on stabilizer formalism, whose main idea is to represent a quantum state as the common eigenstate of a set of mutually commuting operators instead of specifying all amplitudes of the wavefunction[20]. The state time evolution under Clifford unitary as well as measurements are performed by modifying the set of operators correspondingly[21]. Notice that we only need L operators to uniquely represent a L qubit quantum state, which would otherwise require 2^L amplitudes.

To complete the simulation, we also need to sample from the uniform distribution of two-qubit Clifford group. Notice that different group elements will map the operator basis X_1, Z_1, X_2, Z_2 to different sets of two-qubit Pauli operators, and the mapping is a unique representation of the unitary. Therefore we could just iterate over all possible mappings from X_1, Z_1, X_2, Z_2 to two-qubit Pauli operators and keep the mappings that preserve all commutation relations among X_1, Z_1, X_2, Z_2. This way we have explicitly generated all elements in the two-qubit Clifford group and then sampling uniformly from it is trivial. A slightly different approach is to sample directly using an iterative algorithm, as presented in the appendix of this paper[14].

Finally, stabilizer formalism also allows efficient evaluation of the entanglement entropy $S(A)$ for any bipartitions of the system. See these papers[9,14] for more details.

III. ENTANGLEMENT PHASE TRANSITION

Starting from an initial product state with all $L = 256$ qubits being $|0\rangle$, we evolve the state through the random Clifford circuit (Fig. 1) and average over many circuit instances for convergence (number of averages ranges from 100 to 2000, depending on the variance of the result).

Fig. 2 (a) plots the time evolution of the entanglement entropy in the middle of the L qubits, with subsystem A consisting of sites $1 \sim L/2$. From this entanglement dynamics, we could identify features that correspond to an entanglement phase transition at critical measurement rate $p_c \approx 0.16$ (black dashed line). Below the critical rate $p < p_c$ the entanglement entropy grows linearly in time until saturation, while above the critical rate entanglement growth is slower than linear and also saturates at much smaller values.

To study the entanglement scaling, we calculate and plot the steady state entanglement entropy S_A between subsystems $1 \sim |A|$ and $|A| + 1 \sim L$ for $1 \leq |A| \leq 128$ at different measurement rates p (Fig. 2 (b)). For better visualization, each curve is rescaled linearly by the maximum entropy at that measurement rate, so that after rescaling the maximum entropy for different p will always be 1. Below p_c, the entanglement entropy scales linearly with subsystem size which corresponds to a volume-law scaling while above p_c the entanglement entropy saturates to a constant regardless what the subsystem size $|A|$ is, which is a clear feature of 1D area law scaling. When $p < p_c$, the volume law scaling coefficient reduces as p increases which means that at steady state the entropy

saturates to smaller values. Similarly when $p > p_c$, we also see a reduction in entropy with larger p, except now the saturation value doesn't depend on $|A|$. A schematic for the phase diagram and entanglement scaling is shown in Fig. 3.

IV. HIGHER DIMENSIONS

Here we would like to extend the 1D results above to higher dimensions and investigate how the entanglement phase transition behaves. Intuitively, at higher dimensions, the connectivity between qubits is higher and therefore the random unitary circuit could generate entanglement more efficiently than 1D. For example, in the absence of projective measurements, 2D random unitary circuit only takes $O(\sqrt{L})$ time to fully scramble and reach the maximal entanglement volume law scaling, while in 1D the time required is $O(L)$. Therefore we would expect the critical measurement rate p_c to increase at higher dimensions.

A. Two dimension

We again consider a system with $L = 256$ qubits, but now we assume they are located on a 16×16 lattice and the unitary time evolution is generated by 2D random unitary circuits which respect the 2D locality. After reaching the steady state, we map the 2D qubit array into a 1D string for evaluating entanglement entropy so that we could calculate S_A versus $|A|$ along this string and study the entanglement scaling. In one dimension, the actual qubit arrangement gives a natural mapping which also preserves the locality of the interactions. In two dimensions, a raster scan mapping (Fig. 4 (a) ii) from the top-left to bottom-right seems natural. However, the boundary sizes for subsystem A along this mapping are approximately constant (Fig. 4 (a) ii) and therefore not ideal for showing 2D area law scaling. To access entropy for square regions of increasing area, we choose the spiral mapping (Fig. 4 (a) i) instead.

The steady state entropy along the spiral mapping for different measurement rates is shown in Fig. 4 (b). At small p, the entropy satisfies a volume-law scaling: S_A increases linearly with $|A|$ until taking maximal value at $|A| = L/2$. At large p, a zigzag pattern emerges which corresponds to a 2D area law scaling. The corners of the zigzag pattern happen exactly at k^2 where k is an integer representing the edge length for region A and the entropy increases with k because the boundary size is larger. Ideally, area law scaling would generate a series of constant entropy plateaus between site k^2 and $(k+1)^2$ and the extra oscillations in Fig. 4 (b) might be due to the finite size of the system. Exactly identity the critical measurement rate p_c is a bit difficult since the transition is not very sharp, but a reasonable estimate by looking at the shape of the curves suggests that p_c might be between 0.18 and 0.24, which indeed seems to be higher than 1D.

B. All-to-all coupling

Now we will consider an extreme case which is all-to-all coupling. In this case, every qubit could interact with every other qubit randomly and therefore the connectivity is much higher. Another way to interpret this is 1D random unitary circuit without the locality constraint. Every time step, we basically randomly reshuffle the qubits and then evolve the state according to the normal 1D random unitary circuit. The linearly rescaled entanglement entropy across the system is shown in Fig. 4 (c) and the maximal entropy at any given measurement rate (in other word the rescaling factor for each curve in Fig. 4 (c)) is plotted against p in Fig. 4 (d).

As the measurement rate increases, the entropy generated by unitary evolution still reduces. However, even at $p = 0.9$ there's still no clear signature of area law scaling and the steady state entropy always increases with $|A|$ and takes maximum at $L/2$. This suggests that an entanglement phase transition from volume law to area law scaling probably doesn't exist with all-to-all coupling, which is not too surprising because the notion of "boundary" as well as "area" of any subsystem A is not really well defined without the locality of the interaction.

Interestingly, the entanglement phase transition was recently studied from a different perspective as a purification transition[17], where the random unitary circuits with measurements takes a fully mixed state as input and the purity of the output state determines different phases of the transition. Basically above a critical measurement rate, the output state will be pure and below that rate, the output state will stay mixed for an exponentially long time. With this new measure, even all-to-all coupled systems exhibit phase transition behavior[17].

V. CONCLUSION

In this work, we investigated the entanglement phase transition induced by local measurements with a hybrid random Clifford circuit model. Both in 1D and 2D, the steady state entanglement entropy undergoes a phase transition from volume law scaling to area law scaling when the measurement rate exceeds some critical value. In 2D the transition measurement rate seems to be higher than 1D due to the increased qubit connectivity at higher dimensions. We also explored all-to-all coupling where there is no clear signature of the entanglement phase transition.

Measurement induced entanglement phase transition has been interpreted from a quantum error correction point of view: the scrambling dynamics of the random unitary circuit effectively protects quantum information from local measurements[22]. Additionally, analytic theory

of the entanglement phase transition has been developed by finding its equivalence with some statistical mechanics models[23,24]. Furthermore, since entanglement entropy is very difficult to access experimentally, proposing new measures to characterize the phase transition is also an interesting direction[24].

[1] Nicolas Laflorencie. Quantum entanglement in condensed matter systems. *Physics Reports*, 646:1–59, 2016.

[2] Michael Levin and Xiao-Gang Wen. Detecting topological order in a ground state wave function. *Physical review letters*, 96(11):110405, 2006.

[3] Alexei Kitaev and John Preskill. Topological entanglement entropy. *Physical review letters*, 96(11):110404, 2006.

[4] Hui Li and F Duncan M Haldane. Entanglement spectrum as a generalization of entanglement entropy: Identification of topological order in non-abelian fractional quantum hall effect states. *Physical review letters*, 101(1):010504, 2008.

[5] Hong Yao and Xiao-Liang Qi. Entanglement entropy and entanglement spectrum of the kitaev model. *Physical review letters*, 105(8):080501, 2010.

[6] Jens H Bardarson, Frank Pollmann, and Joel E Moore. Unbounded growth of entanglement in models of many-body localization. *Physical review letters*, 109(1):017202, 2012.

[7] Maksym Serbyn, Z Papić, and Dmitry A Abanin. Universal slow growth of entanglement in interacting strongly disordered systems. *Physical review letters*, 110(26):260601, 2013.

[8] Hyungwon Kim and David A Huse. Ballistic spreading of entanglement in a diffusive nonintegrable system. *Physical review letters*, 111(12):127205, 2013.

[9] Adam Nahum, Jonathan Ruhman, Sagar Vijay, and Jeongwan Haah. Quantum entanglement growth under random unitary dynamics. *Physical Review X*, 7(3):031016, 2017.

[10] Adam Nahum, Jonathan Ruhman, and David A Huse. Dynamics of entanglement and transport in one-dimensional systems with quenched randomness. *Physical Review B*, 98(3):035118, 2018.

[11] Tibor Rakovszky, Frank Pollmann, and CW Von Keyserlingk. Sub-ballistic growth of rényi entropies due to diffusion. *Physical review letters*, 122(25):250602, 2019.

[12] Guifré Vidal. Efficient classical simulation of slightly entangled quantum computations. *Physical review letters*, 91(14):147902, 2003.

[13] Yaodong Li, Xiao Chen, and Matthew PA Fisher. Quantum zeno effect and the many-body entanglement transition. *Physical Review B*, 98(20):205136, 2018.

[14] Yaodong Li, Xiao Chen, and Matthew PA Fisher. Measurement-driven entanglement transition in hybrid quantum circuits. *Physical Review B*, 100(13):134306, 2019.

[15] Brian Skinner, Jonathan Ruhman, and Adam Nahum. Measurement-induced phase transitions in the dynamics of entanglement. *Physical Review X*, 9(3):031009, 2019.

[16] Frank Arute, Kunal Arya, Ryan Babbush, Dave Bacon, Joseph C Bardin, Rami Barends, Rupak Biswas, Sergio Boixo, Fernando GSL Brandao, David A Buell, et al. Quantum supremacy using a programmable superconducting processor. *Nature*, 574(7779):505–510, 2019.

[17] Michael J Gullans and David A Huse. Dynamical purification phase transitions induced by quantum measurements. *arXiv preprint arXiv:1905.05195*, 2019.

[18] Daniel Gottesman. The heisenberg representation of quantum computers. *arXiv preprint quant-ph/9807006*, 1998.

[19] Adam Nahum, Sagar Vijay, and Jeongwan Haah. Operator spreading in random unitary circuits. *Physical Review X*, 8(2):021014, 2018.

[20] Michael A Nielsen and Isaac Chuang. Quantum computation and quantum information, 2002.

[21] Scott Aaronson and Daniel Gottesman. Improved simulation of stabilizer circuits. *Physical Review A*, 70(5):052328, 2004.

[22] S Choi, Y Bao, XL Qi, and E Altman. Quantum error correction in scrambling dynamics and measurement induced phase transition. *arXiv preprint arXiv:1903.05124*.

[23] Chao-Ming Jian, Yi-Zhuang You, Romain Vasseur, and Andreas WW Ludwig. Measurement-induced criticality in random quantum circuits. *Physical Review B*, 101(10):104302, 2020.

[24] Yimu Bao, Soonwon Choi, and Ehud Altman. Theory of the phase transition in random unitary circuits with measurements. *Physical Review B*, 101(10):104301, 2020.